Journal of Metals, Materials and Minerals, 35(3), e2351, 2025

Eco-friendly synthesis of flower-like hierarchical structure of CuO NPs for advancing photocatalytic efficiency and antibacterial applications

Yodchai TANGJAIDEBORISUT[1], Paramasivam SHANMUGAM[2,3], Supakorn BOONYUEN[3,*], Govindasamy SIVA[4], Prema YUGALA[5], Joon Ching JUAN[6], Choowin PHANAWANSOMBAT[7], Atchariya PITINTHARANGKUL[7], Seerangaraj VASANTHARAJ[8], Pornpan PUNGPO[9], and Pariya NA NAKORN[1,*]

[1] *Department of Biotechnology, Faculty of Science and Technology, Thammasat University, Pathum Thani 12120, Thailand*
[2] *Department of Biomaterials, Saveetha Dental College and Hospital, SIMATS, Saveetha University, Chennai 600077, Tamil Nadu, India*
[3] *Department of Chemistry Faculty of Science and Technology, Thammasat University, Patumthani, 12121, Thailand*
[4] *Department of Physics, Bannari Amman Institute of Technology, Sathyamangalam 638 401, Tamil Nadu, India*
[5] *Shrewsbury International School Bangkok Riverside, 1922 Charoen Krung Road, Bang Kholaem, Bangkok, 10120, Thailand*
[6] *Nanotechnology & Catalysis Research Centre (NANOCAT), Institute for Advanced Studies (IAS), University of Malaya, Kuala Lumpur, Malaysia*
[7] *Harrow International School Bangkok, 45 Soi Kosum Ruam Chai 14, Don Mueang, Bangkok 10210, Thailand*
[8] *Department of Biotechnology, Hindusthan College of Arts and Science, Coimbatore 641 028, Tamil Nadu, India*
[9] *Department of Chemistry and Center of Excellence for Innovation in Chemistry, Faculty of Science, Ubon Ratchathani University, Ubon Ratchathani 34190, Thailand*

***Corresponding author e-mail**: chemistrytu@gmail.com, pariya@tu.ac.th

Received date:
5 March 2025
Revised date:
20 April 2025
Accepted date:
7 May 2025

Keywords:
CuO NPs;
Flower-like structure;
Photodegradation;
Methylene blue;
Eco-friendly

Abstract

In recent decades, environmental pollution caused by organic dyes and pathogenic microorganisms has posed significant challenges to both ecological and public health. Therefore, the development of multifunctional materials capable of simultaneously degrading dyes and exhibiting antibacterial properties is crucial for effective environmental remediation. Combining photocatalytic dye degradation with antibacterial activity offers a promising approach to address these dual concerns in a single process. The present study investigates the copper oxide nanparticles (CuONPs) were prepared by green synthetic method using bamboo extract for degradation of methylene blue and inactivation of biological pathogens. The green synthesized CuONPs were characterized various spectroscopic and microscopic techniques including XRD, FTIR, TEM, EDS, and UV-DRS analysis. Based on the XRD pattern, the average crystallite size was calculated to be approximately 24 nm. The photocatalytic efficiency of the as prepared CuONPs were examined through degradation of MB under UV-visible light irradiation. The maximum degradation efficiency of 89.12% was achieved by within 150 min. The CuONPs demonstrated significant photocatalytic efficiency, attributed to their excellent charge separation properties. Additionally, to alter the catalyst amount, [MB] and pH to identify optimal degradation conditions. The CuONPs also exhibited remarkable reusability, maintaining over 85% degradation efficiency after five cycles. Furthermore, antibacterial activity was assessed against *Staphylococcus aureus* (S. aureus) and *Escherichia coli* (E. coli) bacteria, with results indicating that the CuONPs were highly toxic to both bacterial strains. This study highlights the potential of CuONPs as sustainable and cost-effective photocatalysts for organic pollutant degradation. The findings suggest promising applications in environmental remediation, including the removal of dyes, antibiotics, and pesticides under UV-visible light irradiation.

1. Introduction

Water pollution caused by dye-contaminated wastewater has become a pressing environmental challenge [1,2]. Industries such as textile dyeing, paper production, food processing, paints, and cosmetics are major contributors, releasing significant quantities of dye-laden effluents into aquatic systems [3,4]. These effluents not only disrupt aquatic ecosystems but also pose serious health risks to humans through the consumption of contaminated aquatic organisms [5,6]. In 2020, global dye production exceeded one million tons, with more than 15% entering industrial wastewater as pollutants [7]. Many of these dyes contain toxic and carcinogenic compounds, making their removal critical for safeguarding both ecosystems and public health [8]. The impact of dyes on aquatic environments is multifaceted [9]. Their vibrant colors obstruct sunlight penetration, reducing photosynthetic activity and adversely affecting aquatic life. Furthermore, the complex molecular structures of dyes, particularly azo dyes, render them highly soluble, resistant to biodegradation, and challenging to remove from wastewater, especially in textile effluents [9]. Traditional treatment methods, including chemical and physical approaches, have limitations

[10,11]. Biological methods, while cost-effective and energy-efficient, struggle with high dye concentrations[12]. Similarly, physicochemical techniques, such as adsorption, filtration, osmosis and coagulation, often produce secondary pollution and incur high operational costs [13]. Therefore, the photodegradation process offers the higher removal efficiencies compared to conventional techniques. Among these, photocatalysis holds particular promise, utilizing solar light to degrade dyes and potentially produce hydrogen gas. However, challenges such as the rapid recombination of photogenerated electron-hole pairs limit the effectiveness of many photocatalytic materials [14,15]. Various types of semiconductor materials including ZnO, CuO, NiO, WO_3, TiO_2 plays an vital role in photocatalytic process [10,16-22]. Especially, copper oxide (CuO) considering significant interest in photodegradation process. CuO is an p-type semiconductor have higher number electron holes (positive charge carriers) than electrons [23]. Syed *et al.* reported the green synthesis of CuONPs from marmelos leaves, the resulting CuONPs act as efficient antibacterial and photocatalysts [24]. The CuONPs is a narrow bandgap semiconduction with a bandgap energy of approximately 1.2 eV to 1.7 eV. Various type of methods is available for the synthesis of CuONPs including physical, chemical and biological method. Among them, the biological method considering greater interest due to production of zero waste [25]. Particularly, the green synthesis methods offer an environmentally friendly alternative for fabricating metal oxide nanoparticles. Manogar et al., developed a copper oxide nanoparticle using green synthesis of method using morinda citriflia leaf extract and produced stable and sphere like structure [26]. Bamboo stem-derived extracts, for example, serve as both reducing and stabilizing agents, enabling the sustainable synthesis of metal oxide nanoparticles through water-based processes. Elias *et al.*, studied the structural and thermal characterization of cellulose and CuO nanocomposites for bamboo plant fiber [27]. These approaches are simple, cost-effective, and do not require specialized equipment, making them ideal for addressing dye pollution in a sustainable manner. For the green synthesis process, bamboo leaf extract considering greater interest, due to richness in bioactive compounds such as flavonoids. It plays a crucial role as a natural and sustainable supporting agent in the synthesis of metal oxide nanoparticles. Flavonoids, with their antioxidant properties and ability to donate electrons, facilitate the reduction of metal ions and stabilize the growing nanoparticles during synthesis [28-30]. Flavonoids plays an crucial role to control the size, morphology and also prevent the agglomeration, thereby ensuring uniformity in the final material. The present study investigates the development of green synthesis of flower-like hierarchical structure of CuO NPs using bamboo plant extract, the obtained CuONPs was utilized for photocatalyst for degradation of organic dyes in contaminated water and antibacterial agents for the *S. aureus* and *E. coli* bacteria. By employing a approach seeks to contribute to the development of sustainable technologies for efficient pollutant removal from water treatment, promoting advancements in environmental protection and prevent aquatic organisms.

2. Methods

2.1 Preparation of plant extract

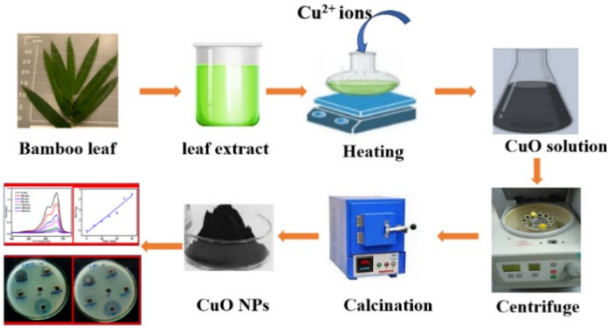

Figure 1. Synthesis of CuONPs using bamboo leaf extract for photocatalytic and antibacterial applications.

The bamboo leaves (Dendrocalamus sericeus Munro) used in this study were collected on September 25, 2024, and the crude extract was prepared using ethanol as the solvent. Initially, 40 g of bamboo leaves were weighed, and 200 mL of ethanol was added to the experimental container. The experiment was divided into two sets based on the extraction method employed. For solvent extraction, the flask containing the bamboo leaves and ethanol was shaken at 150 rpm for 7 days at room temperature. The resulting solution was filtered through Whatman® No. 4 filter paper, and the residue was washed with ethanol to ensure complete extraction. The filtered extract was evaporated under vacuum to remove the solvent. The crude extract was stored in amber glass bottles at 4°C to prevent antioxidant degradation and preserve its bioactivity.

2.2 Synthesis of copper oxide (CuONPs) nanoparticles

CuONPs were synthesized using a co-precipitation method with minor modifications [31]. The synthesis was carried out using 100 mL of bamboo plant extract (1000 ppm), which was mixed with copper nitrate hexahydrate (1 M, 50 mL) in a flask and heated at 60°C on a hot plate for several minutes. Subsequently, 50 mL of 1 M ammonia solution was added dropwise to the reaction mixture, resulting black color precipitate was formed. The solution was stirred continuously at 60°C for 2 h. After complete precipitation, the suspension was centrifuged at 8,000 rpm for 10 min to remove the impurities. The black-colored powder was washed thoroughly twice with distilled water, further purified by centrifugation, and then washed with 100% ethanol to ensure the complete removal of residues and to neutralize the pH. The resulting black-colored powder was dried and calcined at 500°C for 3 h. The synthesized CuONPs were confirmed by XRD, FTIR, and TEM/EDS analyses and were utilized as photocatalysts and antibacterial reagents.

2.3 Photocatalytic study

The photocatalytic activity of bamboo extract derived CuONPs was assessed through degradation of MB under UV-visible light irradiation. In the standard procedure, 10 mg of the catalyst was immersed in a solution containing MB (10 $mg \cdot L^{-1}$). Initially, the balance between adsorption and desorption of MB on the catalyst surface was established by the mixture was stirred at dark condition

for 60 min. Following this, the photocatalytic reaction mixture was exposed to a 500W- Xe lamp as the UV light source. At 30 min intervals, 2.5 mL of the reaction mixture was extracted and remove the catalyst particles was removed by centrifugal process. The concentration of MB was determined by UV-Vis spectrophotometer by measuring the absorption intensity at 665 nm. The photodegradation efficiency was quantified by plotting the ratio of C_0 (initial MB concentration) to C (MB concentration after t_t min) against time (t). All photocatalytic tests were repeated at least twice to confirm the consistency and dependability of the results.

2.4 Antibacterial activity

The antibacterial properties of CuONPs were evaluated against *S. aureus* and *E. coli* using Nutrient Agar medium. Initially, 20 mL of nutrient agar were poured into petri plates and seeded with a 24 h culture. Wells containing *S. aureus 902* and *E. coli 443* were treated with different concentrations of CuONPs (500, 250, 100, and 50 $\mu g \cdot mL^{-1}$). Incubation of the plates was carried out at 37°C for 24 h. The antibacterial activity was evaluated by measuring the zone diameters around the wells [32], with gentamicin as the positive control. The results were analyzed using GraphPad Prism 6.0 software (USA).

3. Results and discussion

The X-ray diffraction (XRD) pattern shown in Figure 2(a) confirms the formation of CuO NPs, as well as their crystal structure and phase purity. The observed diffraction peaks of CuO at 32.47°, 35.58°, 38.75°, 48.81°, 53.27°, 58.24°, 61.24°, 66.23°, 68.05°, 72.12°, and 75.17° correspond to the (110), (002), (111), (202), (020), (127), (113), (022), (220), (222), and (313) planes, which match well with the standard monoclinic CuO structure (JCPDS 80-1916) [33]. The sharp and intense diffraction peaks indicate that the CuO NPs possess good crystallinity. No additional peaks are observed in the XRD pattern, which confirms that the green-synthesized CuO NPs exhibit high phase purity and contain no detectable impurities [34]. Furthermore, using the Debye-scherrer equation ($D = K\lambda/\beta\cos\theta$) to calculate the particle size. The calculated particle size was found to be approximately 24 nm.

The surface functional groups and formation of Cu-O bond can be identified Fourier transform infrared spectroscopy (FTIR) spectrum, as illustrated in Figure 2(b). The absorption band observed at 539 cm^{-1} corresponds to the Cu-O stretching vibration, which is a strong indication of CuO formation [33]. The broad peak observed at 3500 cm^{-1} to 3200 cm^{-1} can be attributed to the O-H stretching vibrations, likely due to adsorbed water molecules. Further, the other minor bands observed at 1000 cm^{-1} to 1500 cm^{-1} might be associated with residual organic species or other functional groups involved during the formation of CuONPs [35]. The both spectral studies confirms the successful preparations of pure and crystalline CuO NPs.

The green-synthesized CuO NPs were analyzed for surface morphology and particle size using transmission electron microscopy (TEM), as depicted in Figures 3(a-b). Figure 3(a) shows CuO NPs with a well-defined, flower-like hierarchical structure composed of numerous nanosheets, which are uniformly distributed and exhibit a high degree of organization. The low-magnification TEM image in Figure 3(a) indicates that these flower-like nanostructures have dimensions in the submicron range, while the constituent nanosheets appear to be extremely thin. A high-magnification TEM image in Figure 3(b) highlights the intricate details of these nanosheets radiating from a common core, further confirming the hierarchical flower-like morphology. Furthermore, the crystalline nature of the CuO NPs was confirmed by the Selected Area Electron Diffraction (SAED) pattern shown in Figure 3(c). The obtained SAED pattern exhibits well-defined concentric rings, which correspond to the diffraction planes of monoclinic CuO. These rings are attributed to the (110), (002), (111), (202), (020), and (113) planes, consistent with the XRD results. The sharpness and uniformity of the rings indicate that the green-synthesized CuO NPs possess high crystallinity and a polycrystalline nature. The TEM and SAED analyses clearly establish that the green-synthesized CuO NPs exhibit a hierarchical flower-like morphology composed of thin nanosheets with excellent crystallinity, which could play a significant role in enhancing their functional properties, particularly for photocatalytic and antimicrobial applications.

The elemental composition of the green synthesized CuO NPs were characterized by Energy Dispersive X-ray Analysis (EDAX) as shown in Figure 4. The EDAX spectrum displays prominent peaks corresponding to copper (Cu), oxygen (O), and carbon (C). The high intensity signals for Cu and O confirm the prepared samples containing CuO NPs as a major component in the sample. The elemental composition table reveals that the weight percentages of Cu and O are 75.74% and 12.28%, respectively, which are well matched with the stoichiometric composition of CuO NPs. A small percentage of carbon (11.98%) is also detected, which is due to the presence of residual organic compounds or carbon-based materials from the green synthesis process. Further, the atomic weight percentages of Cu and O were found to be 54.21% and 25.44%, thus evidence supports the formation of CuO. The absence of additional peaks corresponding to other elements indicates the purity of the synthesized CuO NPs.

UV-Vis diffuse reflectance spectroscopy (UV-DRS) was used to examine the optical properties of the green-synthesized CuO NPs, with the related Tauc plot presented in Figure 5(a-b). Figure 5(a) illustrates the absorbance spectrum, indicating that the material exhibits strong absorption in the UV-visible range, particularly below 400 nm [36,37]. This broad absorption spectrum indicates the potential for photocatalytic activity under UV and visible light irradiation, which is effectively degrade the organic pollutant. The slight absorption tail in the visible region further supports the material's ability to utilize light beyond the UV region. Further, to calculate the energy band gap values (E_g) of the CuONPs, the Kubelka-Munk function was employed, and a Tauc plot was constructed, as shown in Figure 5(b). The plot shows $(\alpha h\nu)^{1/2}$ plotted against photon energy $h\nu$, where α denotes the adsorption coefficient and $h\nu$ is the photon energy. The extrapolation of the linear portion of the curve to the x-axis reveals the band gap energy. The calculated energy band gap of the synthesized CuONPs is app 2.04 eV, thus indicated by the dotted line in Figure 5(b). This relatively narrow band gap enhances the photocatalytic efficiency by allowing for effective absorption of visible light, facilitating the generation of electron-hole pairs. The optical properties of the CuONPs are particularly advantageous for enhance the degradation of MB photocatalytic degradation of organic pollutants and antimicrobial properties.

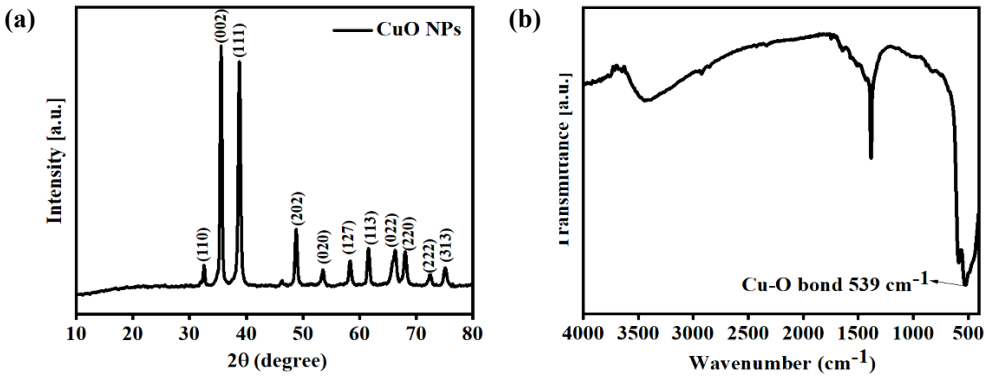

Figure 2. (a) X-ray Diffraction (XRD) patterns, and (b) FTIR spectrum of the CuONPs.

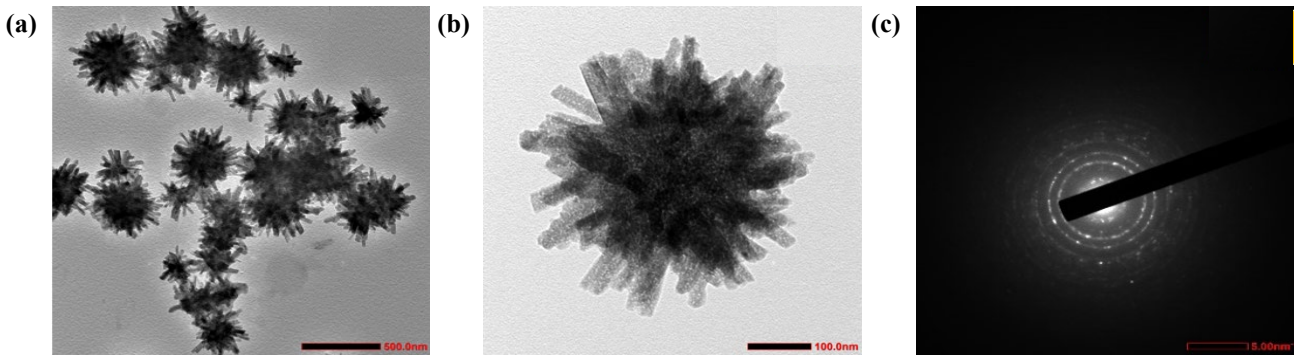

Figure 3. TEM images of CuONPs (a) Low magnification, (b) High magnification, and (c) SAED pattern of the CuONPs.

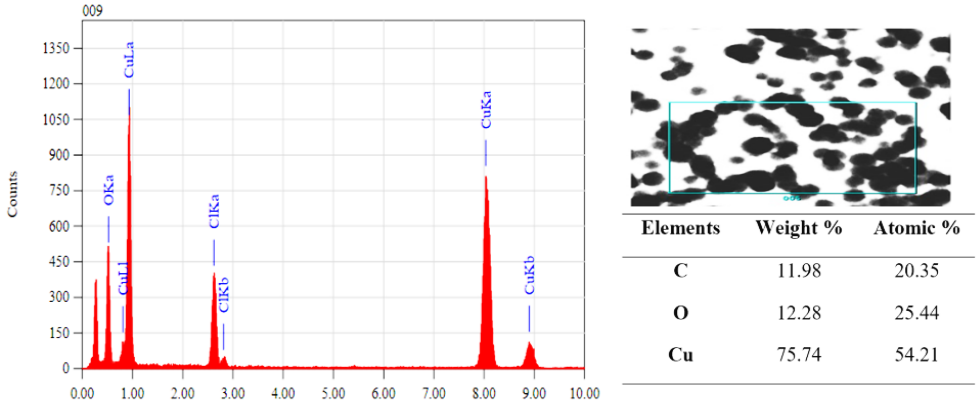

Elements	Weight %	Atomic %
C	11.98	20.35
O	12.28	25.44
Cu	75.74	54.21

Figure 4. Energy-Dispersive X-ray Spectroscopy (EDS) analysis of CuONPs.

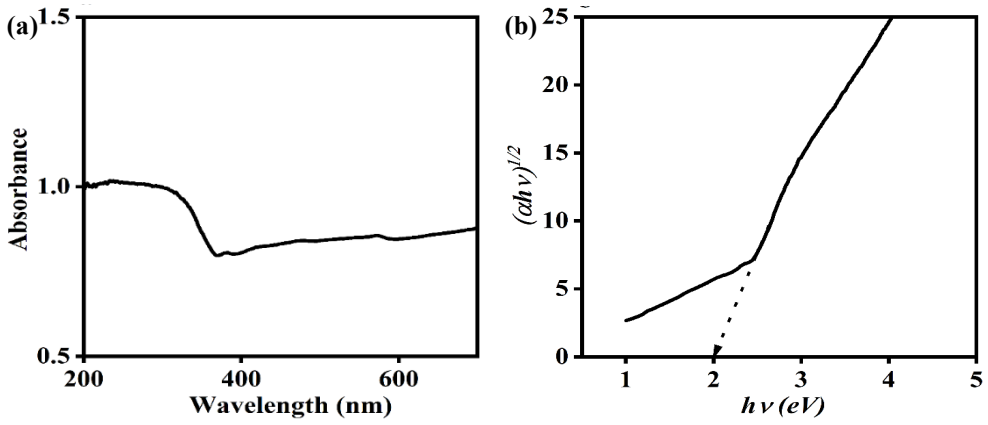

Figure 5. (a) UV-DRS for the CuONPs, and (b) Tauc plot for the CuONPs.

3.1 Photocatalytic activity of CuO NPs against MB dye

The catalytic efficiency of the CuO NPs was evaluated by the degradation of MB dye under UV-visible light irradiation, as shown in Figure 6. Figure 6(a) presents the UV-Vis absorption spectra of MB at different time intervals (0 min to 180 min). The maximum intensity absorption peak was noticed at 664 nm was gradually reduced over time under VLI in the presence of CuO NPs. The complete disappearance of the peak after 180 min provides clear spectral evidence of the excellent photocatalytic efficiency of CuO NPs. Figure 6(b) illustrates the normalized concentration ratio (C/C_0) of MB as a function of irradiation time. The results shows that the concentration of MB significantly decreases over time, with complete degradation achieved within 180 min. This confirms the high photocatalytic efficiency of the green-synthesized CuO NPs. To further investigate the kinetics of the photocatalytic reaction, the obtained results were fitted with pseudo-first-order kinetic model, as illustrated in Figure 6(c). The plot of $-ln(C/C_0)$ vs. time (T) shows a linear relationship, with reaction coefficient values close to unity, thus reveals that MB degradation follows pseudo first-order reaction kinetics. Additionally, reusability is a crucial factor for photocatalytic applications. After each photocatalytic cycle, the CuO NPs were recovered by filtration followed by centrifugation to remove impurities and then dried. The same photocatalytic reaction was repeated for five consecutive cycles, as displayed in Figure 6(d). The degradation efficiency decreased slightly from 89.12% in the first cycle to 84.28% in the fifth cycle. This minor decline in efficiency indicates the excellent stability and recyclability of the CuO NPs as a photocatalyst. Overall, the green-synthesized CuO NPs demonstrate efficient photocatalytic activity for MB degradation, high degradation efficiency, favorable kinetic behavior, and excellent reusability. These results highlight the potential of CuO NPs as a promising candidate for wastewater treatment and environmental remediation applications. The photocatalytic efficiency of the CuO NPs was compared with various photocatalysts from similar studies in previous publications, as displayed in Table 1.

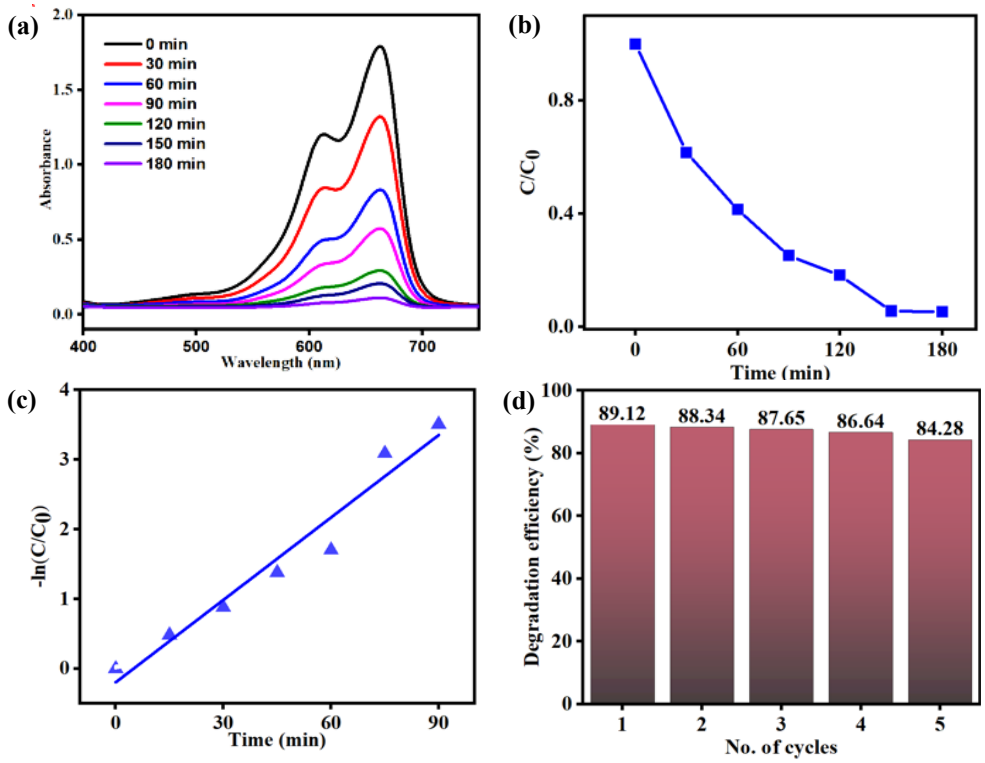

Figure 6. (a) UV-Visible spectra of the photodegradation of MB over CuONPs, (b) Assessment of the photodegradation of MB over CuONPs, (c) Pseudo-first order kinetic plots for the photodegradation of MB dye, and (d) Recycling efficiency of the degradation of MB over CuONPs.

Table 1 Assessment for photocatalytic response by various nanoparticles against MB dye in comparison to the present study.

Natural reducing agent	Photocatalysts	Efficiency %	Light irradiation	Time [min]	Reference
Zizyphus jujuba	NiO	65.5	Sun light	180	[38]
Cyphomandra betacea	SnO_2	85.1	Uv light	70	[39]
Eichhoria crassipes	ZnO	72	Sun light	60	[40]
Moringa oleifera	Fe_3O_4	20	UV-light	60	[41]
Moringa oleifera	Co_3O_4	93.44	UV-light	180	[42]
Jasmin sambac	CuO	97	Sun light	210	[43]
Bamboo leaf	CuO	89.17	Xe lamp	180	This work

3.2 Factors affecting the photocatalytic activity

The PCA of the catalyst was evaluated under varying conditions, including catalyst dosage, dye concentration, and pH, as illustrated in Figure 7(a-c). The optimum photocatalytic activity was observed at a catalyst dosage of 30 mg, [MB] 20 ppm, and a neutral pH of 7, as determined through the kinetic process.

3.2.1 Effect of catalyst dosage

Catalyst dosage plays a vital role in enhancing the photocatalytic degradation of MB dye on the catalyst surface. Figure 7(a) depicts how varying the dosage of CuO NPs affects the degradation of MB dye (20 mg·L^{-1}). An increase in catalyst dosage led to an improvement in degradation efficiency, with a maximum efficiency of 89.12% observed at 30 mg of catalyst after 180 min. This improvement can be attributed to the increased availability of active sites and a higher number of photogenerated electron-hole pairs, which enhance the degradation process [44,45]. However, further increasing the catalyst dosage to 40 mg resulted in a slight decrease in efficiency (79.12%). This reduction is likely due to light scattering and reduced light penetration caused by the excess catalyst in the solution, which hinders the activation of photocatalysts. Additionally, the CuO NPs may aggregate and scavenge the –OH radicals formed during the photocatalytic reaction, further limiting the degradation efficiency.

3.2.2 Effect of [MB]

The influence of the initial MB dye concentration on photocatalytic degradation in the presence of CuO NPs under UV-visible light was investigated. Various dye concentrations (20 mg·L^{-1} to 50 mg·L^{-1}) were treated with 30 mg of CuO NPs under optimized conditions, and the degradation efficiency is presented in Figure 7(b). The results indicate an inverse relationship between dye concentration and degradation efficiency. At the lowest concentration (20 ppm), the degradation efficiency reached a maximum of 89.12%. However, as the dye concentration increased to 30 ppm, 40 ppm, and 50 ppm, the efficiency declined to 77.36%, 68.34%, and 52.64%, respectively. This decrease can be attributed to the limited availability of active sites on the catalyst surface and reduced light penetration into the solution, both of which hinder the degradation process [46].

3.2.3 Effect of pH

The pH is a key factor in influencing the surface charge and the aggregation behavior within the reaction system, thereby affecting the degradation of dye molecules. As illustrated in Figure 7(c), variations in pH notably impacted the photocatalytic performance. The degradation efficiency was lowest in a highly acidic medium, with a value of 24.24% at pH 1, and gradually increased with rising pH levels. At neutral pH (pH 7), the efficiency reached 89.12%. Further increases in pH to 11 and 14 resulted in enhanced degradation efficiencies of 93.12% and 98.98%, respectively. The extremely low degradation efficiency in acidic conditions may be attributed to the lack of sufficient hydroxyl ions (OH^-) needed to generate hydroxyl radicals ($^{\bullet}OH$), which are critical for the photocatalytic reaction [47]. Conversely, at higher pH levels, the degradation efficiency increased significantly due to the electrostatic interaction between the cationic MB dye and the negatively charged hydroxyl ions present on the surface of CuO NPs. This interaction promotes the generation of hydroxyl radicals, which accelerate the breakdown of dye molecules, thereby enhancing the photocatalytic efficiency in basic media.

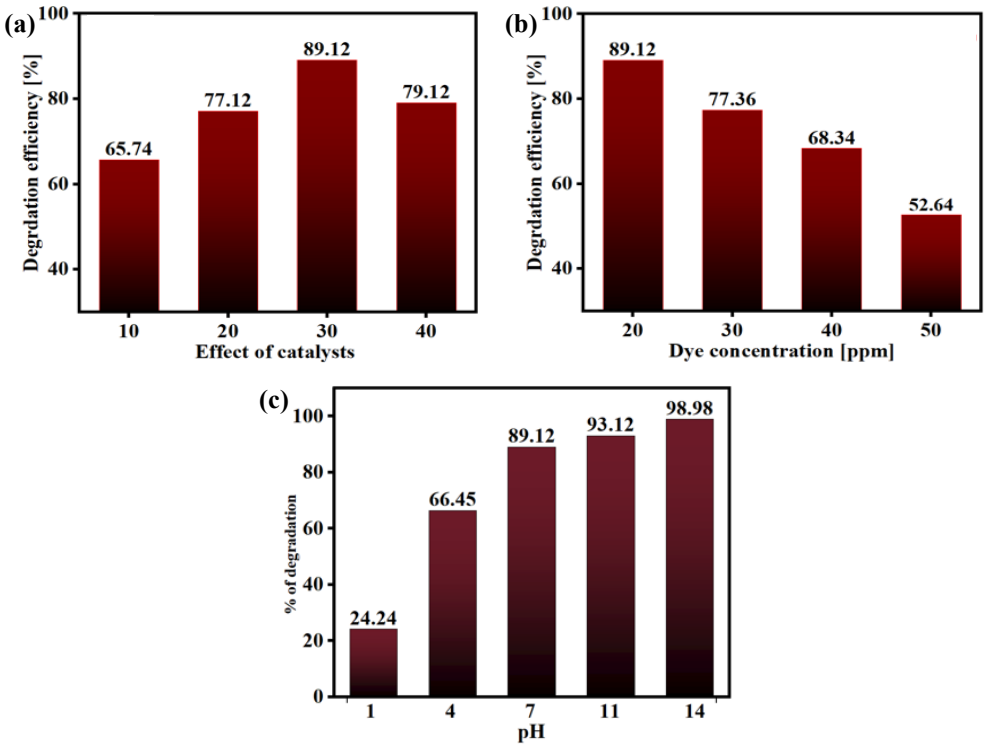

Figure 7. Factors influencing the photodegradation of MB over CuONPs (a) catalyst dosage, (b) effect of initial dye concentration, and (c) effect of pH.

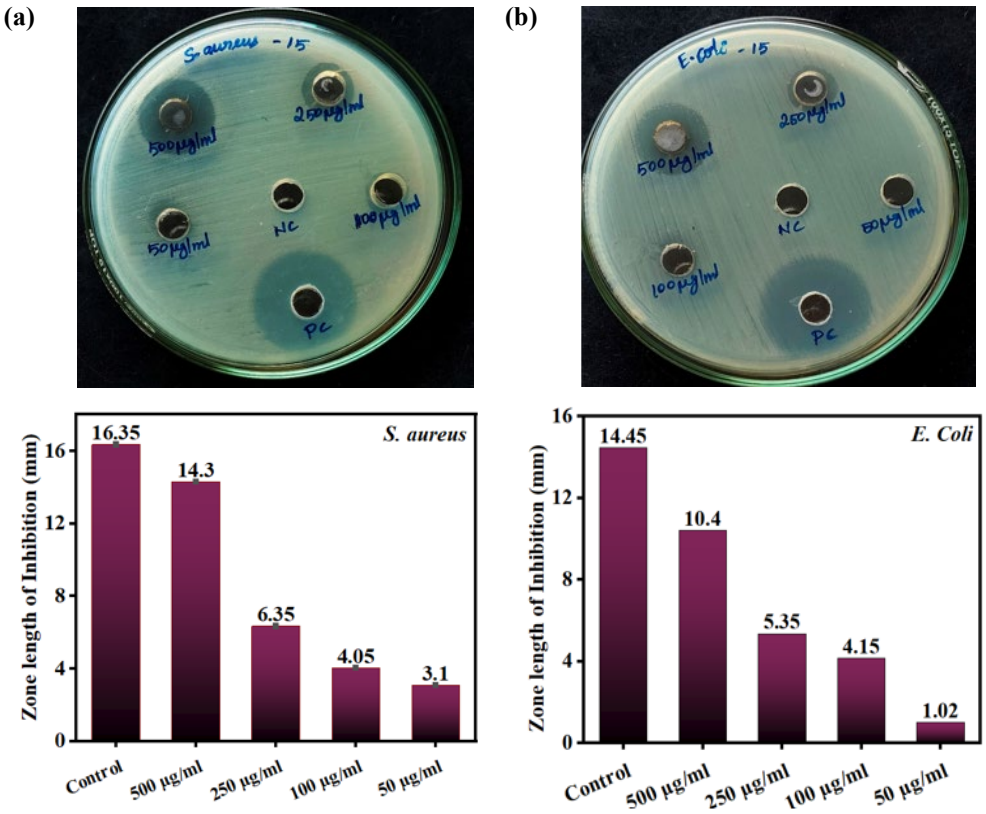

Figure 8. Antibacterial efficiency of the CuONPs (a) *S. aureus,* (b) *E. Coli.*

3.3 Antibacterial activities

The antibacterial activity of green-synthesized CuONPs was evaluated against *S. aureus* and *E. coli* using the disk diffusion method, as illustrated in Figure 8(a-b), respectively. The results demonstrated a dose-dependent antibacterial effect, where higher concentrations of CuONPs produced larger zones of inhibition. For *S. aureus* (Figure 8(a)), the largest inhibition zone was observed at 500 µg·mL^{-1}, measuring 14.3 mm, followed by 6.35 mm at 250 µg·mL^{-1}. In contrast, lower concentrations, such as 100 µg·mL^{-1} and 50 µg·mL^{-1}, displayed reduced inhibition zones of 4.05 mm and 3.1 mm, respectively, with the minimal response occurring at 50 µg·mL^{-1} (3.1 mm). A similar trend was observed for *E. coli* (Figure 8(b)), where the maximum zone of inhibition, 10.4 mm, was recorded at 500 µg·mL^{-1}, followed by 5.35 mm at 250 µg·mL^{-1}. As the concentration decreased to 100 µg·mL^{-1} and 50 µg·mL^{-1}, the inhibition zones were significantly reduced to 4.15 mm and 1.02 mm, respectively. The smallest zone of inhibition was recorded at 50 µg·mL^{-1} (1.02 mm). The results clearly indicate that green-synthesized CuONPs exhibit significant antibacterial activity, with higher concentrations demonstrating greater efficacy. Notably, *S. aureus* exhibited higher sensitivity to CuONPs compared to *E. coli*, as evidenced by the larger inhibition zones at equivalent concentrations. This difference in sensitivity can be attributed to variations in bacterial cell wall structure. Gram-positive bacteria (*S. aureus*) possess a thicker peptidoglycan layer, which may enhance the interaction and uptake of nanoparticles, leading to membrane disruption and the generation of reactive oxygen species (ROS). Conversely, Gram-negative bacteria (*E. coli*) contain an additional outer membrane that acts as a barrier, restricting the penetration of CuONPs and, consequently, reducing their antibacterial efficacy. The obtained results concluded that, the green-synthesized CuONPs demonstrate promising potential as effective antimicrobial agents. Their antibacterial activity is likely mediated through multiple mechanisms, including ROS generation, membrane integrity disruption, and interactions with intracellular components, ultimately causing bacterial cell death [48,49]. These findings highlight the efficacy of CuONPs, particularly against Gram-positive bacteria, and underscore their potential applications in combating bacterial infections.

4. Conclusions

This study demonstrates the successful synthesis of CuO NPs using bamboo plant extract, showcasing their dual functionality in photocatalytic dye degradation and antibacterial activity. The CuONPs achieved a high degradation efficiency of 89.12% for MB dye under UV-visible and retained over 85% efficiency after five consecutive cycles, highlighting their excellent stability and reusability. Furthermore, the CuONPs exhibited significant anti-bacterial properties, effectively inhibiting the growth of *S. aureus* and *E. coli*. These findings under-score the potential of CuONPs as sustainable, cost-effective materials for environmental remediation, offering a promising solution for the removal of organic pollutants and pathogens. The demonstrated multi-functionality and environmental applicability suggest their broader use in addressing pollution challenges involving dyes, antibiotics, and pesticides under UV-visible light conditions.

Acknowledgements:

This research is supported by Thailand Science and Innovation (TSRI) Fundamendal Fund, fiscal year 2025. This study was supported by Thammasat University Research Fund, Contract No. TUFT 022/2568. and partially supported by the Fundamental Fund, Contract No.TUFF 13/2568. Further, the author was greatly acknowledgment to FOODMATRIX GLOBAL CO., LTD, raw materials and chracterization support.

Authors contribution

Yodchai Tangjaideborisut: Methodology, Data Curation; **Paramasivam Shanmugam**: Supervision, Writing—Original Draft, Writing—Review & Editing; **Supakorn Boonyuen**: Conceptualization, Methodology, Formal Analysis, Investigation; **Govindasamy Siva**: Formal Analysis, Data Curation; **Prema Yugala**: Validation, Software, Methodology; **Joon Ching Juan**: Writing—Review & Editing; **Choowin Phanawansombat**: Writing—Review & Editing; **Atchariya Pitintharangkul**: Investigation, Resources, Writing—Review & Editing; **Seerangaraj Vasantharaj**: Resources, Validation, Data Curation; **Pornpan Pungpo**: Validation, Writing—Review & Editing; **Pariya Na Nakkom**: Validation, Formal Analysis, Writing—Review & Editing.

References

[1] S. Subhapriya, and P. Gomathipriya, "Green synthesis of titanium dioxide (TiO_2) nanoparticles by *Trigonella foenum-graecum* extract and its antimicrobial properties," *Microbial Pathogenesis*, vol. 116, pp. 215-220, 2018.

[2] E. T. Helmy, E. M. Abouellef, U. A. Soliman, and J. H. Pan, "Novel green synthesis of S-doped TiO2 nanoparticles using *Malva parviflora* plant extract and their photocatalytic, anti-microbial and antioxidant activities under sunlight illumination," *Chemosphere*, vol. 271, p. 129524, 2021.

[3] D. R. Eddy, D. Rahmawati, M. D. Permana, T. Takei, Solihudin, Suryana, A. R. Noviyanti, and I. Rahayu, "A review of recent developments in green synthesis of TiO_2 nanoparticles using plant extract: Synthesis, characterization and photocatalytic activity," *Inorganic Chemistry Communications*, vol. 165, p.112531, 2024.

[4] R. Saini, and P. Kumar, "Green synthesis of TiO_2 nanoparticles using *Tinospora cordifolia* plant extract & its potential application for photocatalysis and antibacterial activity," *Inorganic Chemistry Communications*, vol. 156, p. 111221, 2023.

[5] N. S. Pavithra, K. N. Manukumar, R. Viswanatha, and G. Nagaraju, "Combustion-derived CuO nanoparticles: Application studies on lithium-ion battery and photocatalytic activities," *Inorganic Chemistry Communications*, vol. 130, p. 108689, 2021.

[6] H. Siddiqui, M. S. Qureshi, and F. Z. Haque, "Biosynthesis of flower-shaped CuO nanostructures and their photocatalytic and antibacterial activities," *Nano-Micro Letters*, vol. 12, p. 29, 2020.

[7] M. D. Khan, A. Singh, M. Z. Khan, S. Tabraiz, and J. Sheikh, "Current perspectives, recent advancements, and efficiencies of various dye-containing wastewater treatment technologies," *Journal of Water Process Engineering*, vol. 53, 103579, 2023.

[8] S. K. Saini, A. K. Dubey, P. Pant, B. N. Upadhyay, and A. Choubey, "Study of laser drilled hole quality of yttria stabilized zirconia," *Lasers in Manufacturing and Materials Processing*, vol. 4, pp. 121-135, 2017.

[9] S. Dutta, S. Adhikary, S. Bhattacharya, D. Roy, S. Chatterjee, A. Chakraborty, D. Banerjee, A. Ganguly, S. Nanda, and P. Rajak, "Contamination of textile dyes in aquatic environment: Adverse impacts on aquatic ecosystem and human health, and its management using bioremediation," *Journal of Environmental Management*, vol. 353, p. 120103, 2024.

[10] U. P. S. Prabhakar, P. Shanmugam, S. Boonyuen, L. P. Chandrasekar, R. Pothu, R. Boddula, A. B. Radwan, and N. Al-Qahtani, "Non-covalent functionalization of surfactant-assisted graphene oxide with silver nanocomposites for highly efficient photocatalysis and anti-biofilm applications," *Materials Science for Energy Technologies*, vol. 7, pp. 205-215, 2024.

[11] P. Shanmugam, S. Boonyuen, Y. Tangjaideborisu, P. Na Nakorn, S. Tantayanon, R. Pothu, and R. Boddula, "Anthocyanin rich-berry extracts coated magnetic Fe_3O_4 bionanocomposites and their antibacterial activity," *Inorganic Chemistry Communications*, vol. 156, p. 111291, 2023.

[12] B. Murugan, M. Z. Rahman, I. Fatimah, J. Anita Lett, J. Annaraj, N. H. M. Kaus, M. A. Al-Anber, and S. Sagadevan, "Green synthesis of CuO nanoparticles for biological applications," *Inorganic Chemistry Communications*, vol. 155, p. 111088, 2023.

[13] S. Parameswaran, R. Bakkiyaraj, P. Shanmugam, S. Boonyuen, and T. Venugopal, "Investigation of biological efficacy assessment of cobalt-doped cerium oxide nanocomposites against pathogenic bacteria, fungi, and lung cancer cells," *Materials Chemistry and Physics*, vol. 321, p.129496, 2024.

[14] B. Abhishek, A. Jayarama, A. S. Rao, S. S. Nagarkar, A. Dutta, S. P. Duttagupta, S. S. Prabhu, and R. Pinto, "Challenges in photocatalytic hydrogen evolution: Importance of photocatalysts and photocatalytic reactors," *International Journal of Hydrogen Energy*, vol. 81, pp. 1442-1466, 2024.

[15] W. Dong, C. Du, Y. Zhang, J. Cao, J. Jiang, L. Zhou, G. Yu, Y. Zou, H. Peng, R. Yan, and Y. Yang, "Enhanced carrier separation and photocatalytic degradation of oxytetracycline via S-scheme MIL-53(Fe)/FeOCl heterojunction composites with peroxydisulfate activation," *Journal of Environmental Chemical Engineering*, vol. 13, p. 115024, 2025.

[16] P. Shanmugam, M. Gopalakrishnan, S. M. Smith, A. Luengnaruemitchai, S. Kheawhom, and S. Boonyuen, "Enhanced photocatalytic performance of magnetically reclaimable N-doped g-C_3N_4/Fe_3O_4 nanocomposites for efficient tetracycline degradation," *Nano-Structures & Nano-Objects*, vol. 40, p. 101392, 2024.

[17] C. Boonwan, T. Rojviroon, O. Rojviroon, R. Rajendran, S. Paramasivam, R. Chinnasamy, S. Ansar, S. Boonyuen, and R. Songprakorp, "Micro-nano bubbles in action: AC/TiO_2 hybrid photocatalysts for efficient organic pollutant degradation and antibacterial activity," *Biocatalysis and Agricultural Biotechnology*, vol. 61, p. 103400, 2024.

[18] S. G. Eswaran, H. Narayan, and N. Vasimalai, "Reductive photocatalytic degradation of toxic aniline blue dye using green synthesized banyan aerial root extract derived silver

nanoparticles," *Biocatalysis and Agricultural Biotechnology*, vol. 36, p. 102140, 2021.

[19] I. Fatimah, Y. Syu'aib, G. D. Ramanda, F. Kooli, S. Sagadevan, and W.-C. Oh, "Facile synthesis of highly active and reusable NiO/montmorillonite photocatalyst for tetracycline removal by photocatalytic oxidation," *Inorganic Chemistry Communications*, vol. 172, p. 113731, 2025.

[20] X. He, T. Jin, M. Wang, A. Huang, and L. Li, "Fabrication and characterization of hierarchically macroporous Al_2O_3 ceramic supported ZnO/ZnS photocatalyst," *Ceramics International*, vol. 51, no. 1, pp. 1247-1258, 2025

[21] M. Rakshita, A. A. Sharma, P. P. Pradhan, K. a. K. Durga Prasad, M. Srinivas, and D. Haranath, "Fabrication and characterization of rare earth-free nanophosphor based devices for solid-state lighting applications," *Materials Advances*, 2025.

[22] K. A. K. D. Prasad, S. Puranjay, M. Rakshita, A. A. Sharma, P. P. Pradhan, K. U. Kumar, R. R. Kumar, and D. Haranath, "Simple and Cost-effective synthesis of a rare-earth free long afterglow phosphor for dark visual markings, *Journal of Fluorescence*, vol. 35, pp. 867-875, 2025.

[23] S. Prakash, N. Elavarasan, A. Venkatesan, K. Subashini, M. Sowndharya, and V. Sujatha, "Green synthesis of copper oxide nanoparticles and its effective applications in Biginelli reaction, BTB photodegradation and antibacterial activity," *Advanced Powder Technology*, vol. 29, pp. 3315-3326, 2018.

[24] S. G. Ali, U. Haseen, M. Jalal, R. A. Khan, A. Alsalme, H. Ahmad, and H. M. Khan, "Green synthesis of copper oxide nanoparticles from the leaves of aegle marmelos and their antimicrobial activity and photocatalytic activities," *Molecules*, vol. 28, p. 7499, 2023.

[25] S. kazemi, A. Hosseingholian, S.D. Gohari, F. Feirahi, F. Moammeri, G. Mesbahian, Z. S. Moghaddam, and Q. Ren, "Recent advances in green synthesized nanoparticles: From production to application," *Materials Today Sustainability*, vol. 24, p. 100500, 2023.

[26] M. Priya, R. Venkatesan, S. Deepa, S. S. Sana, S. Arumugam, A. M. Karami, A. A. Vetcher, and S.-C. Kim, "Green synthesis, characterization, antibacterial, and antifungal activity of copper oxide nanoparticles derived from Morinda citrifolia leaf extract," *Scientific Reports*, vol. 13, p.18838, 2023.

[27] E. E. Elemike, D. Onwudiwe, and W. Ivwurie, "Structural and thermal characterization of cellulose and copper oxide modified cellulose obtained from bamboo plant fibre," *SN Applied Sciences*, vol. 2, no. 10, p. 1725, 2020.

[28] S. kazemi, A. Hosseingholian, S. D. Gohari, F. Feirahi, F. Moammeri, G. Mesbahian, Z. S. Moghaddam, and Q. Ren, "Recent advances in green synthesized nanoparticles: from production to application," *Materials Today Sustainability*, vol. 24, p. 100500, 2023.

[29] S. Ying, Z. Guan, P. C. Ofoegbu, P. Clubb, C. Rico, F. He, and J. Hong, "Green synthesis of nanoparticles: Current developments and limitations," *Environmental Technology & Innovation*, vol. 26, p. 102336, 2022.

[30] M. Zahra, H. Abrahamse, and B. P. George, "Flavonoids: Antioxidant powerhouses and their role in nanomedicine," *Antioxidants*, vol. 13, p. 922, 2024

[31] P. Koteeswari, S. Sagadevan, I. Fatimah, A. Kassegn Sibhatu, S. Izwan Abd Razak, E. Leonard, and T. Soga, "Green synthesis and characterization of copper oxide nanoparticles and their photocatalytic activity," *Inorganic Chemistry Communications*, vol. 144, p. 109851, 2022.

[32] R. C. Ngullie, P. Shanmugam, M. H. Mahmoud, U. P. S. Prabhakar, M. L. Aruna Kumari, and M. Shaheer Akhtar, "Fabrication of biomass derived carbon supported iron oxide composites for antibacterial and antifungal activity," *Materials Letters*, vol. 312, p.131664, 2022.

[33] Z. Alhalili, "Green synthesis of copper oxide nanoparticles CuO NPs from *Eucalyptus Globoulus* leaf extract: Adsorption and design of experiments," *Arabian Journal of Chemistry*, vol. 15, p. 103739, 2022.

[34] W. M. Rangel, R. A. A. Boca Santa, and H. G. Riella, "A facile method for synthesis of nanostructured copper (II) oxide by coprecipitation," *Journal of Materials Research and Technology*, vol. 9, pp. 994-1004, 2020.

[35] S. Parameswaran, P. Shanmugam, R. Bakkiyaraj, and T. Venugopal, "Fabrication and assessment of CuO and NiO-infused MnO_2 nanocomposites: Characterization, methylene blue degradation, and antibacterial efficacy," *Journal of Molecular Structure*, vol. 1303, p. 137560, 2024

[36] V. Usha, S. Kalyanaraman, R. Thangavel, and R. Vettumperumal, "Effect of catalysts on the synthesis of CuO nanoparticles: Structural and optical properties by sol-gel method," *Superlattices and Microstructures*, vol. 86, pp. 203-210, 2015.

[37] J. K. Sharma, M. S. Akhtar, S. Ameen, P. Srivastava, and G. Singh, "Green synthesis of CuO nanoparticles with leaf extract of *Calotropis gigantea* and its dye-sensitized solar cells applications," *Journal of Alloys and Compounds*, vol. 632, pp. 321-325, 2015.

[38] A. Miri, F. Mahabbati, A. Najafidoust, M. J. Miri, and M. Sarani, "Nickel oxide nanoparticles: Biosynthesized, characterization and photocatalytic application in degradation of methylene blue dye," *Inorganic and Nano-Metal Chemistry*, vol. 52, no. 1, pp. 122-131, 2022.

[39] G. Elango, and S. M. Roopan, "Efficacy of SnO_2 nanoparticles toward photocatalytic degradation of methylene blue dye," *Journal of Photochemistry and Photobiology B: Biology*, vol. 155, pp. 34-38, 2016.

[40] O. A. Zelekew, S. G. Aragaw, F. K. Sabir, D. M. Andoshe, A. D. Duma, D.-H. Kuo, X. Chen, T. D. Desissa, B. B. Tesfamariam, G. B. Feyisa, H. Abdullah, E. T. Bekele, and F. G. Aga, "Green synthesis of Co-doped ZnO via the accumulation of cobalt ion onto Eichhornia crassipes plant tissue and the photocatalytic degradation efficiency under visible light," *Materials Research Express*, vol. 8, p. 025010, 2021.

[41] N. Madubuonu, S. O. Aisida, A. Ali, I. Ahmad, T. Zhao, S. Botha, M. Maaza, and F. I. Ezema, "Biosynthesis of iron oxide nanoparticles via a composite of *Psidium guavaja-Moringa oleifera* and their antibacterial and photocatalytic study," *Journal of Photochemistry and Photobiology B: Biology*, vol. 199, p. 111601, 2019.

[42] S. Savitha, S. Surendhiran, K. S. G. Jagan, A. Karthik, B. Kalpana, and R. Senthilmurugan, "Evaluation of the physico-chemical characteristics and photocatalytic activity of cobalt

oxide nanoparticles derived from Moringa seed extract," *Journal of Materials Science: Materials in Electronics*, vol. 34, p. 89, 2023.

[43] S. Nouren, I. Bibi, A. Kausar, M. Sultan, H. Nawaz Bhatti, Y. Safa, S. Sadaf, N. Alwadai, and M. Iqbal, "Green synthesis of CuO nanoparticles using *Jasmin sambac* extract: Conditions optimization and photocatalytic degradation of methylene blue dye," *Journal of King Saud University - Science*, vol. 36, no. 3, p. 103089, 2024.

[44] D. Zhang, S. Lv, and Z. Luo, "A study on the photocatalytic degradation performance of a $[KNbO_3]_{0.9}$-$[BaNi_{0.5}Nb_{0.5}O_{3-\delta}]_{0.1}$ perovskite, *RSC Advances*, vol. 10, pp. 1275-1280, 2020.

[45] A. Gnanaprakasam, V. M. Sivakumar, and M. Thirumarimurugan, "Influencing parameters in the photocatalytic degradation of organic effluent via nanometal oxide catalyst: A review," *Indian Journal of Materials Science*, vol. 2015, p. 601827, 2015.

[46] J. Zhao, C. Chen, and W. Ma, "Photocatalytic degradation of organic pollutants under visible light irradiation," *Topics in Catalysis*, vol. 35, pp. 269-278, 2005.

[47] M. MuthuKathija, S. Muthusamy, R. I. Khan, M. S. M. Badhusha, K. Rajalakshmi, V. Rama, and Y. Xu, "Photocatalytic degradation of methylene blue dye using biogenic copper oxide nanoparticles and its degradation pathway analysis," *Inorganic Chemistry Communications*, vol. 161, p.111929, 2024.

[48] N. S. Ahmad, N. Abdullah, and F. M. Yasin, "Toxicity assessment of reduced graphene oxide and titanium dioxide nanomaterials on gram-positive and gram-negative bacteria under normal laboratory lighting condition," *Toxicology Reports*, vol. 7, pp. 693-699, 2020.

[49] P. R. More, S. Pandit, A. D. Filippis, G. Franci, I. Mijakovic, and M. Galdiero, "Silver nanoparticles: Bactericidal and mechanistic approach against drug resistant pathogens, *Microorganisms*, vol. 11, p. 369, 2023.